



# ENVIRONMENTAL HEALTH PERSPECTIVES

<http://www.ehponline.org>

## Assessing Temporal and Spatial Patterns of Observed and Predicted Ozone in Multiple Urban Areas

Heather Simon, Benjamin Wells, Kirk R. Baker,  
and Bryan Hubbell

<http://dx.doi.org/10.1289/EHP190>

Received: 16 October 2015

Revised: 17 December 2015

Accepted: 27 April 2016

Published: 6 May 2016

**Note to readers with disabilities:** *EHP* will provide a [508-conformant](#) version of this article upon final publication. If you require a 508-conformant version before then, please contact [ehp508@niehs.nih.gov](mailto:ehp508@niehs.nih.gov). Our staff will work with you to assess and meet your accessibility needs within 3 working days.



# Assessing Temporal and Spatial Patterns of Observed and Predicted Ozone in Multiple Urban Areas

Heather Simon, Benjamin Wells, Kirk R. Baker, and Bryan Hubbell

U.S. Environmental Protection Agency, Office of Air Quality Planning and Standards, Research  
Triangle Park, North Carolina, USA

**Address correspondence to** Heather Simon, 109 TW Alexander Dr., Research Triangle Park,  
NC 27711 USA. Telephone: 919-541-1803. E-mail: [simon.heather@epa.gov](mailto:simon.heather@epa.gov)

**Running title:** Temporal and spatial O<sub>3</sub> patterns in 3 urban areas

**Acknowledgments:** The authors would like to thank Norm Possiel, Amy Lamson, Kimber  
Scavo, James Hemby, Kristen Bremer, and Michael Koerber at the US EPA for their thoughtful  
review and comments on this article.

**Disclaimer:** Although this paper has been reviewed by EPA and approved for publication, it  
does not necessarily reflect EPA's policies or views.

**Competing financial interests:** The authors declare no actual or potential competing financial  
interest.

## Abstract

**Background:** Ambient monitoring data show spatial gradients in O<sub>3</sub> across urban areas. NO<sub>x</sub> emissions reductions will likely alter these gradients. Epidemiological studies often use exposure surrogates that may not fully account for impacts of spatially and temporally changing concentrations on population exposure.

**Objectives:** Examine impact of large NO<sub>x</sub> decreases on spatial and temporal O<sub>3</sub> patterns and implications on exposure.

**Methods:** We used a photochemical model to estimate O<sub>3</sub> response to large NO<sub>x</sub> reductions. We derived time series of 2006-2008 O<sub>3</sub> concentrations consistent with 50% and 75% NO<sub>x</sub> emissions reduction scenarios in three urban areas (Atlanta, Philadelphia, and Chicago) at each monitor location and spatially interpolated O<sub>3</sub> to census tract centroids.

**Results:** We predict that low O<sub>3</sub> concentrations increase and high O<sub>3</sub> concentrations decrease in response to NO<sub>x</sub> reductions within an urban area. O<sub>3</sub> increases occurred across larger areas for the seasonal mean metric compared to the regulatory metric (annual 4<sup>th</sup> highest daily 8-hour maximum) and were located only in urban core areas. O<sub>3</sub> always decreased outside the urban core (e.g., at locations of maximum local ozone concentration) for both metrics and decreased within the urban core in some instances. NO<sub>x</sub> reductions lead to more uniform spatial gradients and diurnal and seasonal patterns and cause seasonal peaks in mid-range O<sub>3</sub> concentrations to shift from mid-summer to earlier in the year.

**Conclusions:** These changes have implications for how O<sub>3</sub> exposure may change due to NO<sub>x</sub> reductions and are informative in the design of future epidemiology studies and risk assessments.

## Introduction

Exposure to ozone ( $O_3$ ) is known to cause negative health effects in humans (U.S. EPA 2013). Many areas in the United States currently experience  $O_3$  concentrations that exceed the National Ambient Air Quality Standards (NAAQS) (<http://www3.epa.gov/ozonepollution/maps.html>). Although there have been substantial emission reductions of  $O_3$  precursors and as a result peak  $O_3$  concentrations have decreased, some areas are expected to continue to exceed the 8-hr  $O_3$  NAAQS in the future (U.S. Environmental Protection Agency 2014a).

Nitrogen oxide ( $NO_x$ ) and volatile organic compound (VOC) emissions react in the atmosphere through complex non-linear chemical reactions when meteorological conditions are favorable to form ground level  $O_3$  (Seinfeld and Pandis 2012). Specifically,  $NO_x$  participates in both  $O_3$  formation and destruction chemical pathways so the net impact of  $NO_x$  emissions on  $O_3$  concentrations depends on the relative abundances of  $NO_x$ , VOC, and sunlight as well as the temporal and spatial scales being examined. Emissions sources of  $NO_x$  and VOC, and the resulting  $O_3$  vary seasonally, diurnally, and spatially. Spatial differences exist from rural to urban, city to city, and even within a given urban area (Marshall et al. 2008). In locations with high concentrations of nitric oxide (NO), one component of  $NO_x$ ,  $O_3$  can become artificially suppressed due to direct reactions of NO with  $O_3$ . These reactions also result in production of other oxidized nitrogen species, which form  $O_3$  away from the emission source location while the wind transports the air mass thus contributing to elevated  $O_3$  downwind (Cleveland and Graedel, 1979). As a result of this chemistry, decreasing  $NO_x$  and VOC emissions generally decrease  $O_3$  at times and locations in which concentrations are high (Simon et al. 2013). In limited circumstances, reductions in

NO<sub>x</sub> emissions can lead to O<sub>3</sub> increases in the immediate vicinity of highly concentrated NO<sub>x</sub> sources, while these same emissions changes generally lead to lower O<sub>3</sub> downwind over longer timescales (Cleveland and Graedel, 1979; Sillman 1999; Murphy et al. 2007; Xiao et al. 2010; Kelly et al. 2015). As emissions of both NO<sub>x</sub> and VOC decrease from sources that have unique temporal and spatial attributes (e.g., power plant NO<sub>x</sub> and mobile source NO<sub>x</sub> and VOC) it is important to understand how O<sub>3</sub> formation regimes vary over different temporal and spatial scales to understand how O<sub>3</sub> concentrations may change as the result of these emissions reductions.

Spatial and temporal variability in pollutant concentrations are a key input to studies evaluating associations between air quality and human health. In the past, epidemiological studies linking O<sub>3</sub> with human health impacts have used ambient measurements in various ways to match against health outcomes. Some studies have used spatially averaged O<sub>3</sub> concentrations for an entire urban area to link with short-term (Smith et al. 2009; Zanobetti and Schwartz 2008) and long-term (Jerrett et al. 2009) mortality. Other studies have used the O<sub>3</sub> monitor closest to the residence of the human subjects (Bell 2006). The use of an average “composite” monitor masks both spatial and temporal heterogeneity that exist in an urban area. Using the nearest monitor may provide a better spatial match but does not fully consider daily activity patterns. Given the spatial and temporal heterogeneity in O<sub>3</sub> and human activity patterns that place a subject in different places at different times of the day, it is potentially important to match activity with a realistic heterogeneous representation of O<sub>3</sub> concentrations. This is true both for conducting epidemiology studies of O<sub>3</sub> health outcomes, and also in the application of the results of those studies in risk and health impact assessments. To the extent that reductions in NO<sub>x</sub> and VOC emissions change the temporal

and spatial patterns of O<sub>3</sub>, use of a spatially averaged O<sub>3</sub> concentration may mask how population-weighted O<sub>3</sub> exposures change.

Recent risk assessments conducted to inform the U.S. EPA review of the O<sub>3</sub> NAAQS included application of results from both controlled human exposure studies and observational epidemiology studies (U.S. EPA 2014b). Estimates of risk based on controlled human exposure studies evaluated changes in the risk of 10 and 15 percent lung function decrements, and used an exposure-response model that is more responsive to changes in exposure when maximum daily 8-hr average (MDA8) O<sub>3</sub> is above 40 ppb. In contrast, estimates of risk based on application of results from epidemiology studies used linear, no-threshold concentration-response functions, so an incremental change in O<sub>3</sub> impacted total risk equally, regardless of the starting level of O<sub>3</sub>. As a result, the epidemiology-based risk estimates could be quite sensitive to the patterns of O<sub>3</sub> responses to NO<sub>x</sub> reductions, while the risk estimates based on controlled human exposure studies reflected the changes that occurred at the higher O<sub>3</sub> concentrations.

Given the complex nature of O<sub>3</sub> chemistry and emissions source mixes in a given urban area, photochemical grid models provide a credible tool for evaluating responsiveness to emissions changes and have been used extensively for O<sub>3</sub> planning purposes in the past (Cai et al. 2011; Hogrefe et al. 2011; Kumar and Russell 1996; Simon et al. 2012). Here, we used a photochemical grid model applied in three different urban areas to illustrate O<sub>3</sub> temporal and spatial patterns and how those patterns may change due to reduced precursor emissions. Model-predicted changes in O<sub>3</sub> were aggregated using several metrics to show how spatial heterogeneity depends on the O<sub>3</sub> metric analyzed and how the type of aggregation used can mute the spatial variability in O<sub>3</sub> response to emissions changes.

## Methods

### City selection and monitoring data

Three major urban areas (Philadelphia, Atlanta, and Chicago) were selected for evaluation based on the spatial coverage of the local ambient monitoring network and because they demonstrate different types of spatial O<sub>3</sub> patterns and responses to emissions changes (U.S. EPA 2014b). In addition, the photochemical model performed well in these cities (U.S. EPA 2014b). For each urban area, all ambient monitoring sites within the Combined Statistical Area (CSA) were included in the analysis as well as any additional monitoring sites within a 50 km buffer of the CSA boundary. Hourly average O<sub>3</sub> data from these ambient monitoring sites for years 2006 - 2008 were obtained from EPA's Air Quality System (AQS) database (<http://www2.epa.gov/aqs>).

### Ambient data adjustments to estimate O<sub>3</sub> distributions under alternate emissions

We applied outputs from a series of photochemical air quality model simulations to estimate how hourly O<sub>3</sub> could change under hypothetical scenarios of 50% and 75% reductions in U.S. anthropogenic NO<sub>x</sub> emissions. Emissions projections from the EPA predict substantial reductions (45%) in U.S. anthropogenic NO<sub>x</sub> between 2007 and 2020 (U.S. EPA 2012). VOC emissions are also expected to decline between 2007 and 2020 by a more modest 20% (U.S. EPA 2012). By evaluating O<sub>3</sub> concentrations at 50% and 75% NO<sub>x</sub> reductions, we were able to look at ozone responses for two scenarios of varying emissions. While the primary focus of this study was on NO<sub>x</sub> reduction scenarios, we also included a more limited evaluation of scenarios where both NO<sub>x</sub> and VOC emissions were reduced by 50% and 75%,

to determine how co-occurring VOC reductions could change patterns of responses to NO<sub>x</sub> reductions.

The methodology for adjusting observed O<sub>3</sub> to scenarios of 50% and 75% NO<sub>x</sub> reductions was adapted from the methods developed in Simon et al. (2013) and U.S. EPA (2014b). However, both of these studies targeted specific air quality goals rather than emissions reduction levels as was investigated here. The methods are described in detail in those documents and are summarized below.

We used the Community Multi-scale Air Quality (CMAQ) model v4.7.1 instrumented with Higher-Order Decoupled Direct Method (HDDM) capabilities to calculate O<sub>3</sub> response to emissions inputs. Details on model set-up and inputs are provided in the Supplemental Material. Model predictions of MDA8 O<sub>3</sub> were compared against monitored values in each of the three cities. Overall the mean bias was 3.7 ppb, 2 ppb, and 1 ppb in Atlanta, Chicago, and Philadelphia. The Pearson correlation (R) was 0.82, 0.86, and 0.88 in the three cities respectively. A seasonal breakout of these performance statistics is provided in the Supplemental Material, Table S1. This model performance is within the range of what has been seen in state-of-the-science ozone modeling reported in recent literature (Simon et al., 2012) and is sufficiently accurate for the purpose of this analysis.

The CMAQ-HDDM system provided outputs of hourly O<sub>3</sub> and hourly sensitivity coefficients at a 12 km × 12 km grid resolution across the contiguous United States. These sensitivities describe a nonlinear (quadratic) O<sub>3</sub> response at a specified time and location to an across-the-board perturbation in NO<sub>x</sub> emissions following Equation 1:

$$\Delta O_{3\ h,l} = -\Delta \varepsilon S_{h,l}^1 + \frac{\Delta \varepsilon^2}{2} S_{h,l}^2 \quad \text{Equation 1}$$

Where  $\Delta O_{3\ h,l}$  is the change in  $O_3$  at hour  $h$  and location  $l$ ,  $\Delta \varepsilon$  is the relative change in  $NO_x$  emissions (e.g. -0.2 represents a 20% reduction in  $NO_x$  emissions) and  $S_{h,l}^1$  and  $S_{h,l}^2$  represent the first and second order  $O_3$  sensitivity coefficients at hour  $h$  and location  $l$ .

Model simulations were performed for seven months in 2007 (January and April-October). This provided  $O_3$  responses over a range of emissions and meteorological conditions and provided information on seasonal variations in the response. To apply the modeled sensitivity coefficients from seven months to three years of ambient measurements (described above), we derived statistical relationships between the modeled sensitivity coefficients and modeled hourly  $O_3$  concentrations using linear regression. Separate linear regressions were created for each monitor location at each hour of the day and for each season resulting in a total of 96 (24 hrs X 4 seasons) linear regressions for the first and second order sensitivity coefficients at each monitor location. The linear regression resulted in statistically significant relationships between ozone concentration and responsiveness to  $NO_x$  emissions reductions for most hours of the day, season and monitoring location combinations. Using these relationships, we were able to determine the first and second order sensitivity coefficients at  $O_3$  monitor locations for every hour of 2006-2008. Finally, we used Equation 1 to predict the change in measured ambient  $O_3$  concentrations for a set change in  $NO_x$  emissions at each monitor location.

An additional complication is introduced when looking at large changes in  $NO_x$  emissions (e.g. 50% and 75%). Past studies have reported that CMAQ-HDDM estimates of  $O_3$  changes are most accurate for emissions perturbations less than 50% (Hakami et al. 2003). To address this, we ran the CMAQ-HDDM model at two distinct emissions levels (2007

emissions and 50% NO<sub>x</sub> conditions) to derive emissions sensitivity coefficients that would occur under different emissions regimes. We then developed a 2-step adjustment methodology in which sensitivity coefficients from each of the simulations were applied over the portion of emissions reductions for which they were most applicable (Simon et al. 2013; U.S. EPA 2014b). The exact point over the emissions reduction glide-path at which the sensitivity was switched differed for each city and was determined by minimizing the least square error between the adjusted O<sub>3</sub> concentrations using the 2-step approach and actual modeled concentrations from “brute force” NO<sub>x</sub> cut simulations. Analysis presented in U.S. EPA (2014b) showed that this 2-step approach was able to replicate O<sub>3</sub> changes for 50% emissions reductions with mean bias between -0.2 and -0.9 ppb and mean absolute error equal to 1 ppb for the three cities evaluated here.

### Spatial Interpolation

In order to better examine spatial patterns in O<sub>3</sub> concentrations and population exposure, we used the Voronoi Neighbor Averaging (VNA) (Gold 1997; Chen et al 2004) method to create spatial fields of the hourly O<sub>3</sub> in each urban area for the observed, 50% NO<sub>x</sub> cut, and 75% NO<sub>x</sub> cut scenarios. We used VNA to interpolate the observed or adjusted hourly concentration data using an inverse distance squared weighting from monitored locations to each census tract centroid within the CSA boundaries of each urban area. The resulting spatial fields provided temporally complete estimates of observed and adjusted hourly O<sub>3</sub> concentrations at refined spatial resolution within each urban area. Previous cross-validation

tests showed that this interpolation method provided good performance at urban scales (U. S. EPA 2014b).

## **Results**

### Predicted spatial changes

We focused on two MDA8 O<sub>3</sub> metrics for our assessment: the annual 4<sup>th</sup> highest MDA8 value averaged over 3 consecutive years, which corresponds to the form and averaging time of the current O<sub>3</sub> NAAQS and represents O<sub>3</sub> concentrations on the highest O<sub>3</sub> days (this is also known as the “design value”, and hereafter is referred to as the regulatory metric), and the May to September mean of the MDA8 (i.e., the seasonal mean metric), which generally tracks well with estimates of epidemiology-based O<sub>3</sub> health risk (U.S. EPA 2014b). Maps of VNA surfaces showing spatial patterns in these metrics for Atlanta, Philadelphia and Chicago are provided in Figures 1 to 3. Left panels show the values based on measured O<sub>3</sub> concentrations, while center and right panels show the changes in these observed values under the 50% and 75% NO<sub>x</sub> cut scenarios respectively.

For the observed scenario, Atlanta has fairly uniform O<sub>3</sub> concentrations (especially for the seasonal average) while Philadelphia and Chicago have sharp spatial gradients due to local O<sub>3</sub> suppression near NO emissions sources in the urban core and subsequent O<sub>3</sub> formation downwind as described in the introduction. When looking at the predicted changes in the two metrics under the 50% and 75% NO<sub>x</sub> cut scenarios, each city displays a different spatial pattern. In Atlanta, large NO<sub>x</sub> reductions are predicted to result in fairly uniform decreases in both O<sub>3</sub> metrics across the CSA although decreases are slightly less pronounced in the urban

core. In Philadelphia, the regulatory metric is predicted to decrease everywhere, while the seasonal mean metric is predicted to slightly increase in a small area of the urban core with 50% NO<sub>x</sub> reductions and decrease in the rest of the CSA. Note that the increases in the seasonal mean tend to occur in locations having lower observed values while decreases tend to occur in locations with higher observed values, resulting in a more uniform spatial gradient. The 75% NO<sub>x</sub> cut scenario predicts decreases in both the regulatory metric and the seasonal mean metric throughout the entire Philadelphia CSA, with decreases being more pronounced in outlying areas. Finally, Chicago displays a third type of response pattern. For the 50% NO<sub>x</sub> reduction scenario, the regulatory metric in Chicago is predicted to slightly increase in the urban core and near Lake Michigan while it decreases in surrounding locations. For the 75% reduction scenario, the regulatory metric shows substantial decreases, while the seasonal mean concentrations still increase in the urban core. The spatial extent of the area where the seasonal mean is predicted to increase is larger than the spatial extent of the area where regulatory metric O<sub>3</sub> is predicted to increase. Figures for spatial patterns in two additional cities (Denver and Sacramento) are provided in the Supplemental Material, Figures S1 and S2. Patterns in Denver resemble those seen in Philadelphia, while patterns in Sacramento most resemble those in Atlanta.

Figures 4 to 7 show populations (2010 census, <http://factfinder.census.gov/faces/nav/jsf/pages/index.xhtml>) of locations predicted to have increasing and decreasing O<sub>3</sub> using the regulatory and seasonal mean metrics in each of the three cities. In general, the least densely populated locations have the highest O<sub>3</sub> and largest decreases in O<sub>3</sub>. Conversely, the most densely populated locations have the lowest O<sub>3</sub> and the smallest decreases, or in some cases increases, in O<sub>3</sub>. Several specific features can be

seen in these histograms. First, in Atlanta and Philadelphia, the entire population lives in locations where the regulatory metric is predicted to decrease. In Chicago, while a small area near the urban core is predicted to have increases in the regulatory metric (50% NO<sub>x</sub> reduction scenario only), the vast majority of the population still lives in locations where the regulatory metric is predicted to decrease. Second, consistent with results in Figure 1, seasonal mean O<sub>3</sub> is predicted to decrease in all locations of Atlanta. In Philadelphia, there is a small area predicted to have increases in seasonal mean O<sub>3</sub> in the 50% NO<sub>x</sub> reduction scenario, but not in the 75% NO<sub>x</sub> reduction scenario. Consequently, a small fraction of the Philadelphia population lives in locations of low but somewhat increasing seasonal mean O<sub>3</sub> in the 50% NO<sub>x</sub> reduction scenario. The net result of these changes in both Atlanta and Philadelphia is that the O<sub>3</sub> distribution is compressed as well as shifted toward lower concentrations for both metrics and in both the 50% and 75% NO<sub>x</sub> cut scenarios (see Supplemental Material, Figures S3 and S4). Finally, compared to the other two cities, Chicago is predicted to have a larger area of increasing seasonal mean O<sub>3</sub>, and consequently, a larger fraction of Chicago residents (55% and 26% for the 50% and 75% NO<sub>x</sub> reduction scenarios respectively) live in those locations (Supplemental Material, Figure S5). Denver and Sacramento results are shown in the Supplemental Material, Figures S6 through S9.

Previous work has shown that VOC emissions reductions can result in lower ambient O<sub>3</sub> levels (Sillman, 1999) and that changes in ambient VOC concentrations can impact how O<sub>3</sub> responds to NO<sub>x</sub> emissions reductions (Chameides et al., 1988). Of the cities we analyzed, previous analysis suggests that anthropogenic VOC emissions reductions will result in the most notable estimated O<sub>3</sub> reductions for the Chicago area (U.S. EPA 2014b). We therefore conducted additional simulations where both anthropogenic VOC and NO<sub>x</sub> were reduced in

Chicago. This resulted in lower regulatory and seasonal metrics than simulations with NO<sub>x</sub> emissions reductions alone (Figures 6 and 7). However, the combined levels of NO<sub>x</sub> and VOC emissions reductions applied here still resulted in some increases in low O<sub>3</sub> in the urban core which shows that the inclusion of VOC reductions does not eliminate the need to understand how heterogeneous O<sub>3</sub> responses to emission reductions can impact exposure.

#### Predicted temporal changes

Figure 8 shows the seasonal pattern in O<sub>3</sub> concentrations at an urban monitor in Philadelphia and a rural downwind monitor over all days with measured values in 2006-2008. As expected, the highest concentrations are observed in the summer months with lower O<sub>3</sub> in the fall and winter. This pattern shifts in the 50% and 75% NO<sub>x</sub> reduction scenarios. First, the monthly maximum concentrations generally decrease while the monthly minimum concentrations increase leading to a compression of the O<sub>3</sub> distribution. Decreases in monthly maximum values are largest during the summer and increases in monthly minimum values are largest in the winter. Second, mid-range O<sub>3</sub> (see top panels of Figure 8) are generally predicted to decrease during the summer and increase in the winter months. The behavior in spring and fall differs at the two locations with increases in those seasons at the urban site, but decreases in spring at the rural site. This leads to a flattening of the seasonal O<sub>3</sub> pattern for both extreme and mid-range O<sub>3</sub> values. Finally, a shift in the seasonal peak for mid-range O<sub>3</sub> concentrations is evident in the 75% NO<sub>x</sub> reduction scenario (compare hatched green and dark blue ribbons in Figure 8 top panels). While observed mid-range concentrations reach their peak in the summer (June, July, August), the mid-range

concentrations in the 75% NO<sub>x</sub> reduction scenario are predicted to be highest in the spring months (March, April, May) with a secondary peak in the fall. This shift is not seen for monthly maximum values. The shifting O<sub>3</sub> seasonal patterns are similar to results reported by Clifton et al. (2014) who use global modeling to predict O<sub>3</sub> increases in winter and decreases in summer on a regional scale. This general phenomenon is corroborated by recent studies analyzing observed O<sub>3</sub> trends corresponding to decreasing NO<sub>x</sub> emissions over the past decade which show wintertime O<sub>3</sub> concentrations have been increasing, while summer concentrations have been decreasing (Simon et al. 2015; Jhun et al. 2014)

Changes in diurnal patterns at these two monitoring sites are shown in the Supplemental Material, Figure S11. Nighttime concentrations are predicted to increase with decreasing NO<sub>x</sub> while daytime concentrations are predicted to decrease. Similar to changes in the seasonal pattern, this generally leads to a flattening out of the diurnal pattern. Increases are more pronounced at the urban monitor, where concentrations are low, than at the rural monitor, where concentrations are high.

Temporal plots for the other four cities show generally similar patterns to what is seen in Philadelphia and can be found in the Supplemental Material, Figures S12 through S19.

### Limitations and Uncertainties

We note several limitations and uncertainties. First, we looked at two scenarios of across-the-board reductions in U.S. anthropogenic NO<sub>x</sub> (and VOC) emissions as case studies to demonstrate how changing emissions could impact O<sub>3</sub> spatial and temporal patterns. Our modeling explored broad regional reductions in NO<sub>x</sub> (and VOC) emissions, and we have not evaluated whether

more spatially focused reductions could be equally effective in reducing peak concentrations, while avoiding increases in O<sub>3</sub> in urban core areas. Future research may explore strategies for mitigating NO<sub>x</sub>-related increases in O<sub>3</sub>. In addition, different sources are likely to reduce their emissions at different rates. This analysis demonstrates how spatial and temporal O<sub>3</sub> patterns and resulting exposure may change with emissions reductions, but does not attempt to predict future emissions levels or the associated effects on O<sub>3</sub>. Second, we applied modeled O<sub>3</sub> responses from 12-km resolution regional model simulations to ambient measurements at O<sub>3</sub> monitors. Although 12-km resolution modeling has generally been shown to capture most features in O<sub>3</sub> response, the variability in predicted O<sub>3</sub> responses can be somewhat muted in comparison to modeling at finer grid resolutions (Cohan et al. 2006). Third, we note that in Philadelphia, the increasing seasonal mean values are only predicted at a single monitor and in Chicago increases in the regulatory metric are only predicted at two monitors. In both cases, there is some uncertainty in the VNA interpolations showing the spatial extent of those increases. Finally, this analysis used seven months of modeling data to represent O<sub>3</sub> responses across three years. The modeling simulated at least one representative month for each season, allowing us to create separate regressions for each site, hour-of-the-day, and season. This enabled us to capture seasonal variability in the response of O<sub>3</sub> to emissions changes. In addition, both meteorology (e.g. ozone conducive conditions) and emissions in 2006 and 2008 may have varied from those in the 2007 modeling year. Therefore the application of regressions based on conditions from 7 months in 2007 to 2006-2008 observations is another source of uncertainty.

## Discussion

The results from this analysis show substantial heterogeneity in O<sub>3</sub> responses within CSAs. This suggests that the composite monitors used in many health studies may mask potentially important aspects of the impact of NO<sub>x</sub> changes on O<sub>3</sub> distributions (changes to high versus low O<sub>3</sub> concentrations, spatial variability, and temporal patterns) and how they relate to total population-weighted exposure.

First, a key observation from our analysis is that for all three areas, O<sub>3</sub> concentrations using the regulatory metric were reduced at locations with the highest concentrations (which are generally the monitors that are targeted when selecting NO<sub>x</sub> or VOC emissions controls). Additionally, monthly maximum O<sub>3</sub> was decreased at both urban and rural sites under the 50% and 75% NO<sub>x</sub> cut scenarios (Figure 8). As noted earlier, some measures of risk, such as the lung function responses derived from controlled human exposures studies, are most sensitive to these reductions in high concentrations and, thus, these risk metrics will show improvement with NO<sub>x</sub> decreases. In contrast, the epidemiology-based risks which are currently equally responsive to changes at low and high concentrations are more ambiguous in response to NO<sub>x</sub> decreases, and ultimately depend on the direction and magnitude of the O<sub>3</sub> change in places with the highest population densities. Since the increases in O<sub>3</sub> almost always occur at low O<sub>3</sub> concentrations, it is increasingly important for health studies to evaluate whether the shape of the concentration-response relationship changes at these lower levels.

Second, spatial gradients of ambient O<sub>3</sub> are evident in each of the urban areas shown, and there is both spatial and temporal heterogeneity in the response of ambient O<sub>3</sub> to NO<sub>x</sub>

decreases. This heterogeneity enhances the importance of understanding where and when people spend their day when linking ambient monitoring data to health outcomes. U.S. EPA (2014b) found that when population exposures to O<sub>3</sub> are modeled using time-activity information, the highest exposures to O<sub>3</sub> occur for children spending a large amount of time outdoors during high O<sub>3</sub> periods, and for adult outdoor workers in high O<sub>3</sub> areas. This suggests that epidemiology studies could be improved and reduce exposure misclassification by providing population exposure surrogates that represent time-activity weighted patterns of O<sub>3</sub> exposure, rather than using simpler spatial averages or single-point measures that assume individuals spend all of their time at a residential location. In addition, time-activity weighted measures of population exposure to O<sub>3</sub> will be better able to capture the changes in spatial and temporal patterns of O<sub>3</sub> that can result from reductions in O<sub>3</sub> precursor emissions to attain the NAAQS.

Third, the model predictions that increases in O<sub>3</sub> are more prevalent in cooler months and decreases are more prevalent in warmer months may be important if activities that lead to increased exposure (such as time spent outdoors) are lower during winter than in summer. Some research suggests that health impacts of O<sub>3</sub> may be lower in cooler months compared to warmer months (Medina-Ramon 2006; Stieb et al. 2009; Strickland et al. 2010). To the extent that O<sub>3</sub> health impacts vary by season, a fuller characterization of exposure patterns may improve understanding of the implications of the predicted changes in seasonal O<sub>3</sub> patterns.

The net impact on health over an entire population will depend on the balance of O<sub>3</sub> changes across high and low population density locations and across the entire O<sub>3</sub> season as well as on the shape of the concentration-response relationship at different concentrations. Our

analysis highlights the potential impacts of NO<sub>x</sub> emissions reductions on spatial and temporal patterns of O<sub>3</sub>. Extensions of this work that elucidate the relationships between population time-activity patterns (as well as potentially affected communities) and these changes in the spatial and temporal patterns of O<sub>3</sub> may allow regulators to consider modifications to NO<sub>x</sub> and VOC reduction plans (e.g., to avoid increases in O<sub>3</sub> at times and locations when they are most likely to result in negative health outcomes).

## References

- Bell M. 2006. The use of ambient air quality modeling to estimate individual and population exposure for human health research: A case study of ozone in the Norther Georgia Region of the United States. *Environment International* 32: 586-593.
- Cai C, Kelly JT, Avise JC, Kaduwela AP, Stockwell WR. 2011. Photochemical modeling in California with two chemical mechanisms: model intercomparison and response to emission reductions. *Journal of the Air & Waste Management Association* 61:559-572.
- Chameides WL, Lindsay RW, Richardson J, Kiang CS. 1988. The role of biogenic hydrocarbons in urban photochemical smog: Atlanta as a case study. *Science* 241: 1473-1475.
- Chen J, Zhao R, Li Z. 2004. Voronoi-based k-order neighbor relations for spatial analysis. *Journal of Photogrammetry and Remote Sensing* 59:60-72.
- Cleveland WS, Graedel TE. 1979. Photochemical air pollution in the Northeastern United States. *Science* 204:1273-1278.
- Clifton OE, Fiore AM, Correa G, Horowitz LW, Naik V. 2014. Twenty-first century reversal of the surface ozone seasonal cycle over the northeastern United States. *Geophysical Research Letters* 41:7343-7350.
- Cohan DS, Hu Y, Russell AG. 2006. Dependence of ozone sensitivity analysis on grid resolution. *Atmospheric Environment* 40:126-135.

Gold C. 1997. Voronoi methods in GIS. In: *Algorithmic Foundation of Geographic Information Systems* (va Kereveld M., Niever gelt, J., Roos, T., Widmayer, P., eds.). *Lecture Notes in Computer Science*, Vol 1340. Berlin: Springer-Verlag, 21-35.

Hakami A, Odman MT, Russell AG. 2003. High-order direct sensitivity analysis of multidimensional air quality models. *Environmental Science & Technology* 37:2442-2452

Hogrefe C, Hao W, Zalewsky E, Ku J-Y, Lynn B, Rosenzweig C, et al. 2011. An analysis of long-term regional-scale ozone simulations over the Northeastern United States: variability and trends. *Atmospheric Chemistry and Physics* 11:567-582.

Jerrett M, Burnett RT, Pope III CA, Ito K, Thurston G, Krewski D, et al. 2009. Long-term ozone exposure and mortality. *New England Journal of Medicine* 360, 1085-1095.

Jhun I, Coull BA, Zanobetti A, Koutrakis P. 2014. The impact of nitrogen oxides concentration decreases on ozone trends in the USA. *Air Quality. Atmosphere & Health* 8:279

Kelly JT, Baker KR, Napelenok SL, Roselle SJ. 2015. Examining single-source secondary impacts estimated from brute-force, decoupled direct method, and advanced plum treatment approaches. *Atmospheric Environment* 111:10-19.

Kumar N, Russell AG. 1996. Multiscale air quality modeling of the northeastern United States. *Atmospheric Environment* 30:1099-1116.

Medina-Ramon M, Zanobetti A, Schwartz, J. 2006. The effect of ozone and PM10 on hospital admissions for pneumonia and chronic obstructive pulmonary disease: A national multicity study. *Am J Epidemiol* 163: 579-588; doi:10.1093/aje/kwj078

- Marshall JD, Nethery E, Brauer M. 2008. Within-urban variability in ambient air pollution: comparison of estimation methods. *Atmospheric Environment* 42:1359-1369.
- Mulholland JA, Butler AJ, Wilkinson JG, Russell AG, Tolbert PE. 1998. Temporal and spatial distributions of ozone in Atlanta: regulatory and epidemiologic implications. *Journal of the Air & Waste Management Association* 48:418-426.
- Murphy JG, Day DA, Cleary PA, Wooldridge PJ, Millet DB, Goldstein AH, et al. 2007. The weekend effect within and downwind of Sacramento – Part 1: Observations of ozone, nitrogen oxides, and VOC reactivity. *Atmospheric Chemistry and Physics* 7:5327-5339.
- Sillman S. 1999. The relation between ozone, NO<sub>x</sub> and hydrocarbons in urban and polluted rural environments. *Atmospheric Environment* 33:1821-1845.
- Simon H, Baker KR, Phillips S. 2012. Compilation and interpretation of photochemical model performance statistics published between 2006 and 2012. *Atmospheric Environment* 61:124-139.
- Simon H, Baker KR, Akhtar F, Napelenok SL, Possiel N, Wells B, et al. 2013. A Direct sensitivity approach to predict hourly ozone resulting from compliance with the National Ambient Air Quality Standard. *Environmental Science & Technology* 47:2304-2313.
- Simon H, Reff A, Wells B, Xing J, Frank N. 2015. Ozone trends across the United States over a period of decreasing NO<sub>x</sub> and VOC emissions. *Environmental Science & Technology* 49:186-195.
- Smith RL, Xu B, Switzer P. 2009. Reassessing the relationship between ozone and short-term mortality in US urban communities. *Inhalation toxicology* 21:37-61.

Stieb DM, Szyszkowicz M, Rowe BH, Leech JA. 2009. Air pollution and emergency department visits for cardiac and respiratory conditions: A multi-city time-series analysis. *Environ Health Global Access Sci Source* 8:25; doi:10.1186/1476-069X-8-25

Strickland MJ, Darrow LA, Klein M, Flanders WD, Sarnat JA, Waller LA, et al. 2010. Short-term associations between ambient air pollutants and pediatric asthma emergency department visits. *Am J Respir Crit Care Med* 182:307-316; doi:10.1164/rccm.200908-1201OC.

U.S. Environmental Protection Agency (EPA). 2012. Regulatory Impact Analysis for the Final Revision to the National Ambient Air Quality Standards for Particulate Matter. Research Triangle Park, NC, EPA-452/R-12-005. <http://www.epa.gov/ttnecas1/regdata/RIAs/finalria.pdf>

U.S. Environmental Protection Agency (EPA), 2013. Integrated Science Assessment of Ozone and Related Photochemical Oxidants (Final Report). Washington, DC, EPA/600/R-10/076F.

U.S. Environmental Protection Agency. 2014a. Regulatory Impact Analysis of the Proposed Revisions to the National Ambient Air Quality Standards for Ground-Level Ozone. Research Triangle Park, NC, EPA-452/P-14-006.

<http://www.epa.gov/ttn/ecas/regdata/RIAs/20141125ria.pdf>.

U.S. Environmental Protection Agency (EPA). 2014b. Health Risk and Exposure Assessment for Ozone, Final Report. U.S. Environmental Protection Agency, Research Triangle Park, NC, EPA-452/R-14-004a. [http://www.epa.gov/ttn/naaqs/standards/ozone/s\\_o3\\_2008\\_rea.html](http://www.epa.gov/ttn/naaqs/standards/ozone/s_o3_2008_rea.html)

Xiao X, Cohan DS, Byun DW, Ngan F. 2010. Highly nonlinear ozone formation in the Houston region and implications for emission controls. *Journal of Geophysical Research* 115:D23309; doi:10.1029/2010JD014435

Zanobetti A, Schwartz J. 2008. Mortality displacement in the association of ozone with mortality: an analysis of 48 cities in the United States. *American Journal of Respiratory and Critical Care Medicine* 177:184-189.

## Figure Legends

Figure 1. Maps showing the 2006-2008 average annual 4<sup>th</sup> highest MDA8 O<sub>3</sub>, the regulatory metric, (ppb, top panels) and May-September mean MDA8 O<sub>3</sub> (ppb, bottom panels) values in Atlanta for observed conditions (left panels), and predicted changes with 50% U.S. NO<sub>x</sub> emissions reductions (center panels) and 75% U.S. NO<sub>x</sub> emissions reductions (right panels). Black boxes show locations of monitoring sites while colored dots show interpolated values at census tract centroids.

Figure 2. Maps showing the 2006-2008 average annual 4<sup>th</sup> highest MDA8 O<sub>3</sub>, the regulatory metric, (ppb, top panels) and May-September mean MDA8 O<sub>3</sub> (ppb, bottom panels) values in Philadelphia for observed conditions (left panels), and predicted changes with 50% U.S. NO<sub>x</sub> emissions reductions (center panels) and 75% U.S. NO<sub>x</sub> emissions reductions (right panels). Black boxes show locations of monitoring sites while colored dots show interpolated values at census tract centroids.

Figure 3. Maps showing the 2006-2008 average annual 4<sup>th</sup> highest MDA8 O<sub>3</sub>, the regulatory metric, (ppb, top panels) and May-September mean MDA8 O<sub>3</sub> (ppb, bottom panels) values in Chicago for observed conditions (left panels), and predicted changes with 50% U.S. NO<sub>x</sub> emissions reductions (center panels) and 75% U.S. NO<sub>x</sub> emissions reductions (right panels). Black boxes show locations of monitoring sites while colored dots show interpolated values at census tract centroids.

Figure 4. Histograms showing population living in Atlanta locations with various 2006-2008 average 4<sup>th</sup> highest MDA8 O<sub>3</sub> (top panels, ppb) and May – September mean MDA8 O<sub>3</sub> (bottom panels, ppb), for observed conditions (left panels), and predicted changes resulting

from 50% U.S. NO<sub>x</sub> emissions reductions (center panels) and 75% U.S. NO<sub>x</sub> reductions (right panels). Colors show the breakdown of each histogram by population density.

Figure 5. Histograms showing population living in Philadelphia locations with various 2006-2008 average 4<sup>th</sup> highest MDA8 O<sub>3</sub> (top panels, ppb) and May – September mean MDA8 O<sub>3</sub> (bottom panels, ppb), for observed conditions (left panels), and predicted changes resulting from 50% U.S. NO<sub>x</sub> emissions reductions (center panels) and 75% U.S. NO<sub>x</sub> reductions (right panels). Colors show the breakdown of each histogram by population density.

Figure 6. Histograms showing population living in Chicago locations with various 2006-2008 average 4<sup>th</sup> highest MDA8 O<sub>3</sub> (top panels, ppb) and May – September mean MDA8 O<sub>3</sub> (bottom panels, ppb), for observed conditions (left panels), and predicted changes resulting from 50% U.S. NO<sub>x</sub> emissions reductions (center panels) and 75% U.S. NO<sub>x</sub> emissions reductions (right panels). Colors show the breakdown of each histogram by population density.

Figure 7. Histograms showing population living in Chicago locations with various 2006-2008 average 4<sup>th</sup> highest MDA8 O<sub>3</sub> (top panels, ppb) and May – September mean MDA8 O<sub>3</sub> (bottom panels, ppb), for observed conditions (left panels), and predicted changes resulting from 50% U.S. NO<sub>x</sub>/VOC emissions reductions (center panels) and 75% U.S. NO<sub>x</sub>/VOC emissions reductions (right panels). Colors show the breakdown of each histogram by population density.

Figure 8. Distribution of 8-hr daily maximum O<sub>3</sub> concentrations in Philadelphia by month at an urban (left panels) and a rural (right panels) monitoring site. Top plots show the

interquartile range (25<sup>th</sup> to 75<sup>th</sup> percentile values) across all days in each month. Bottom plots show minimum and maximum values across all days in each month.

Figure 1.

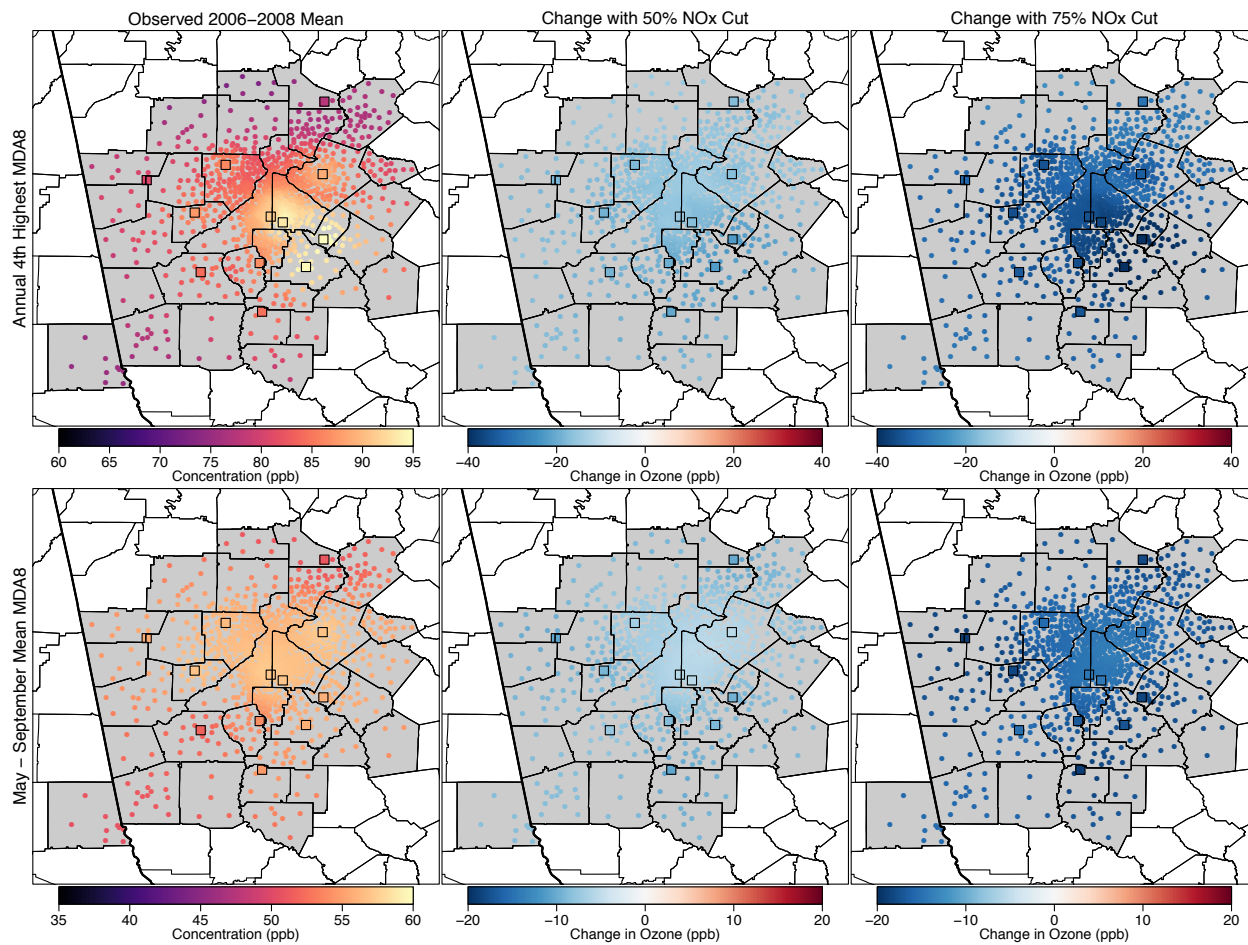


Figure 2.

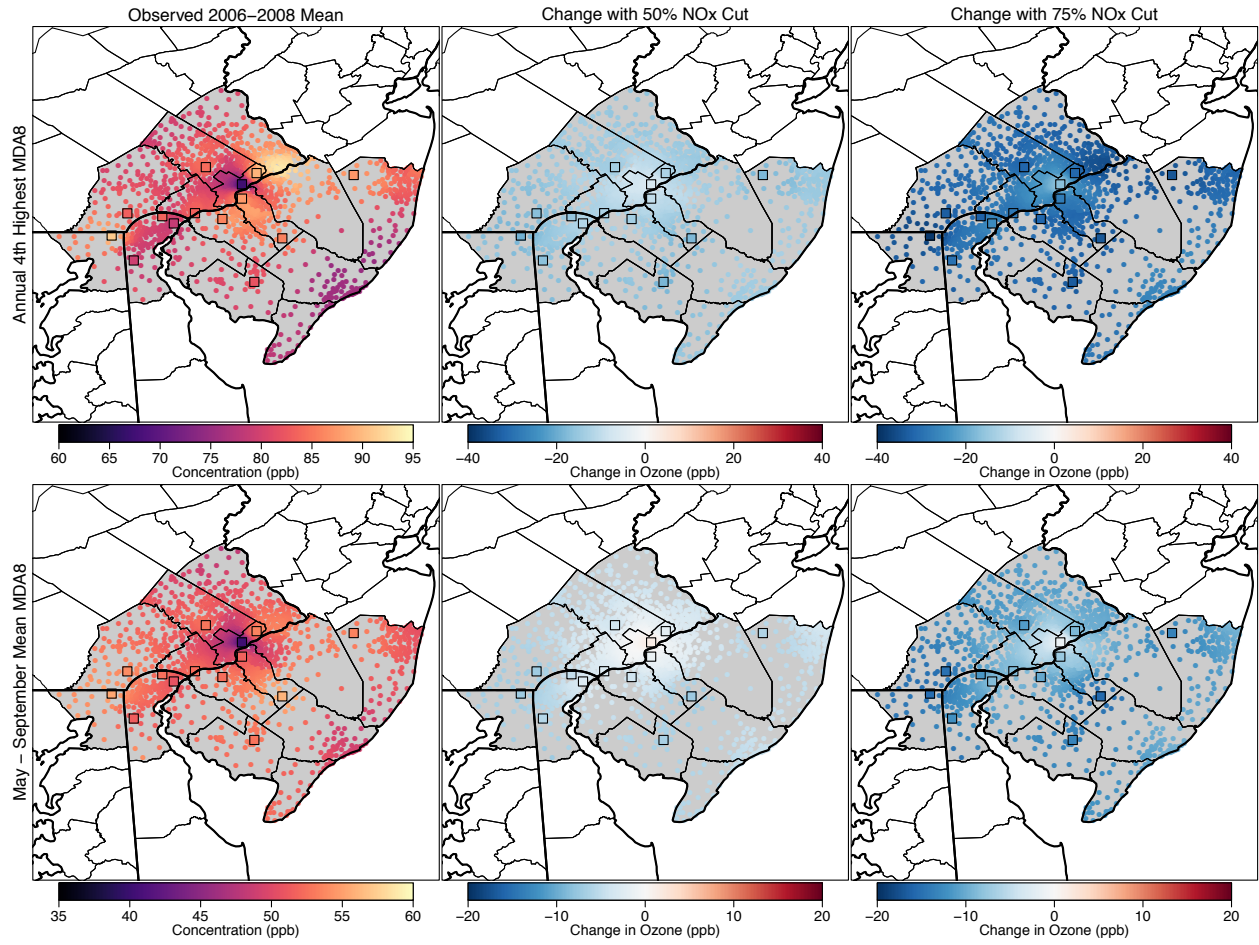


Figure 3.

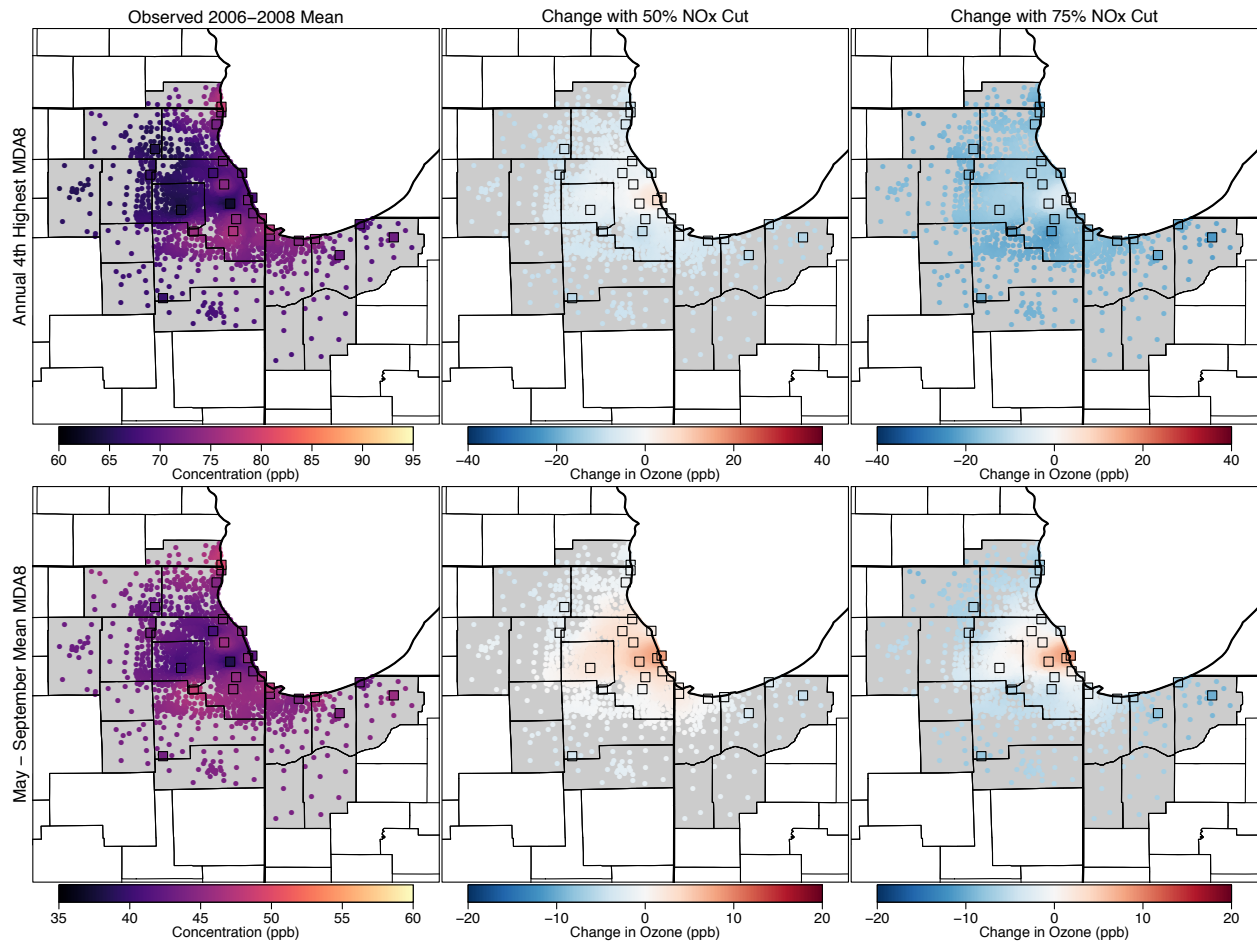


Figure 4.

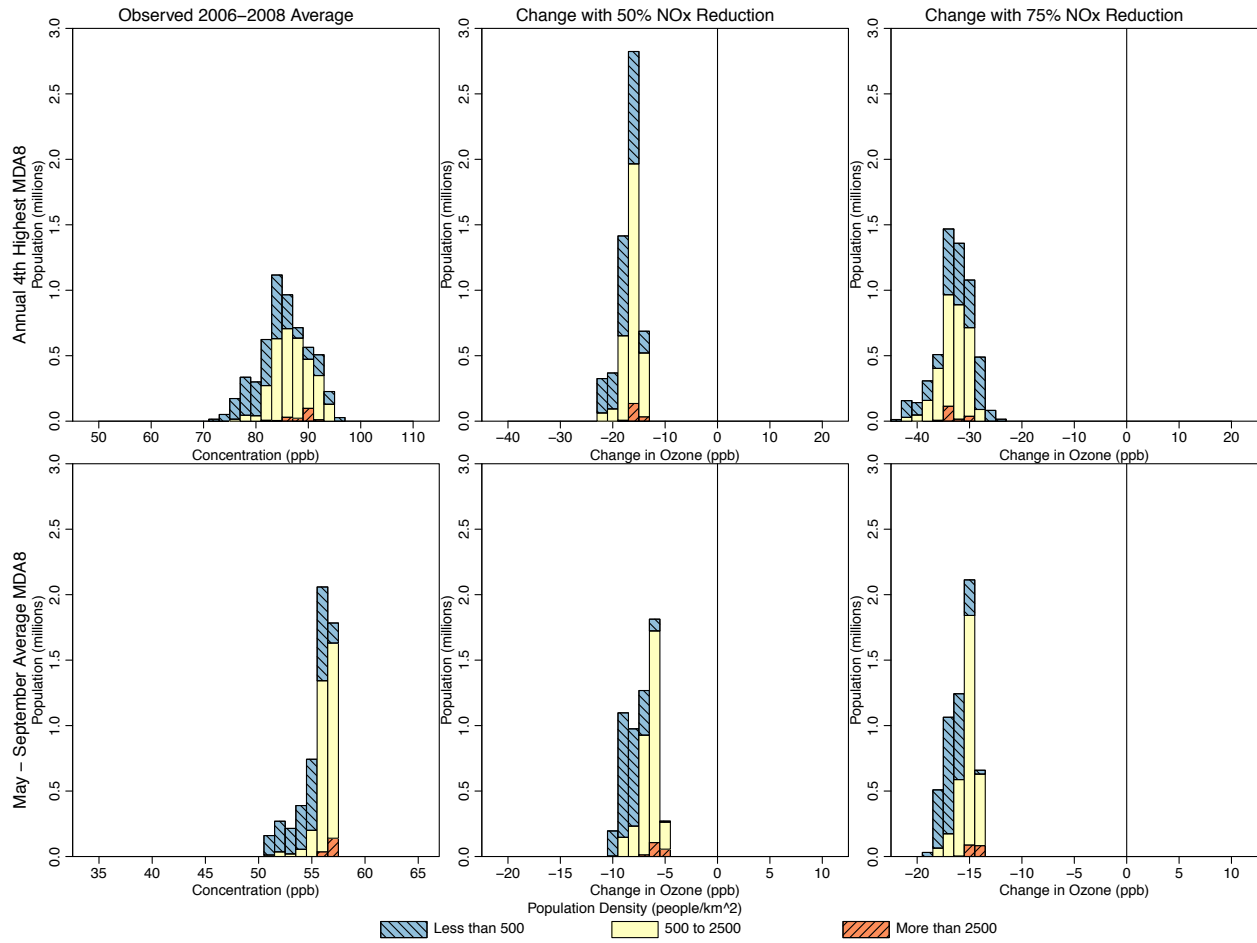


Figure 5.

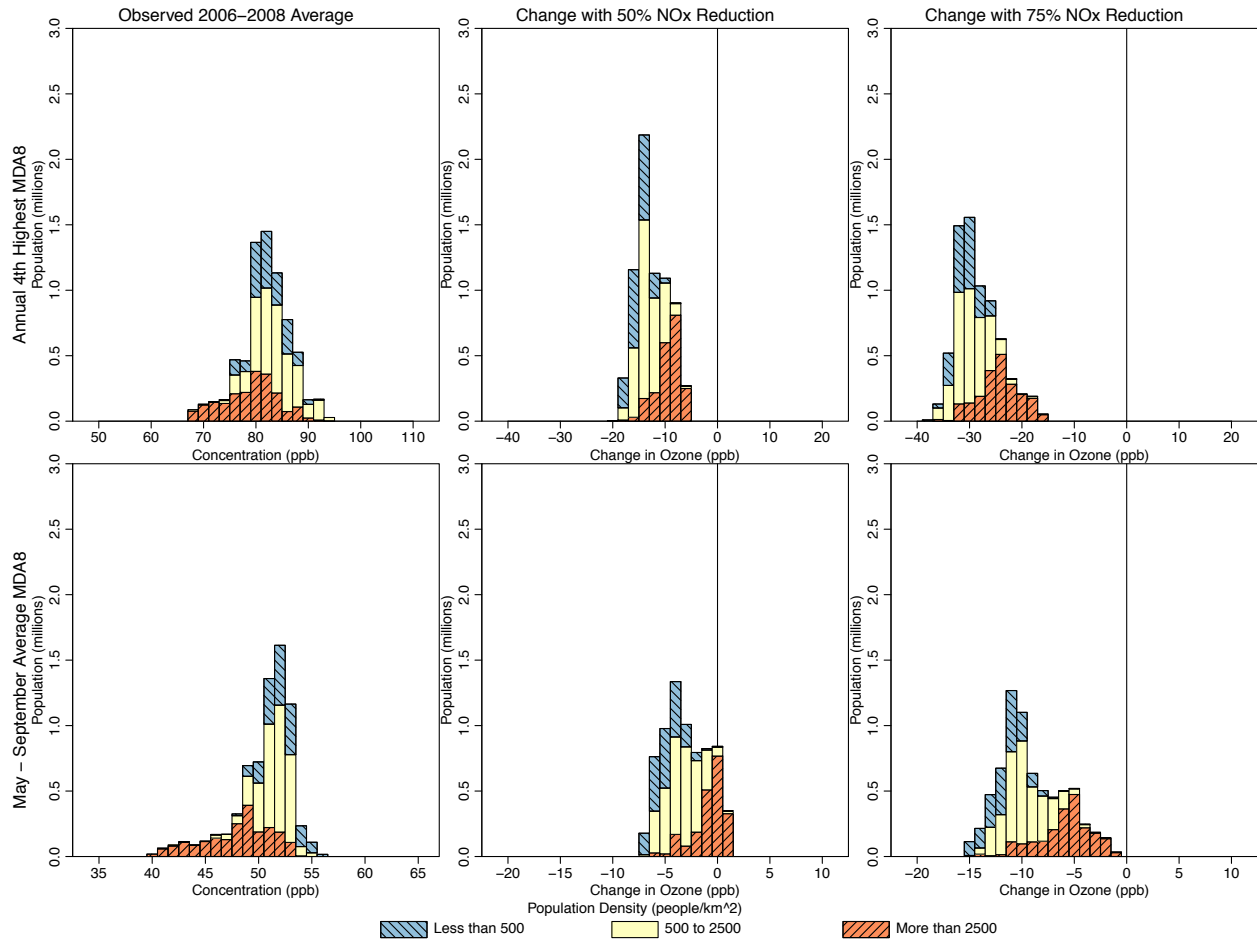


Figure 6.

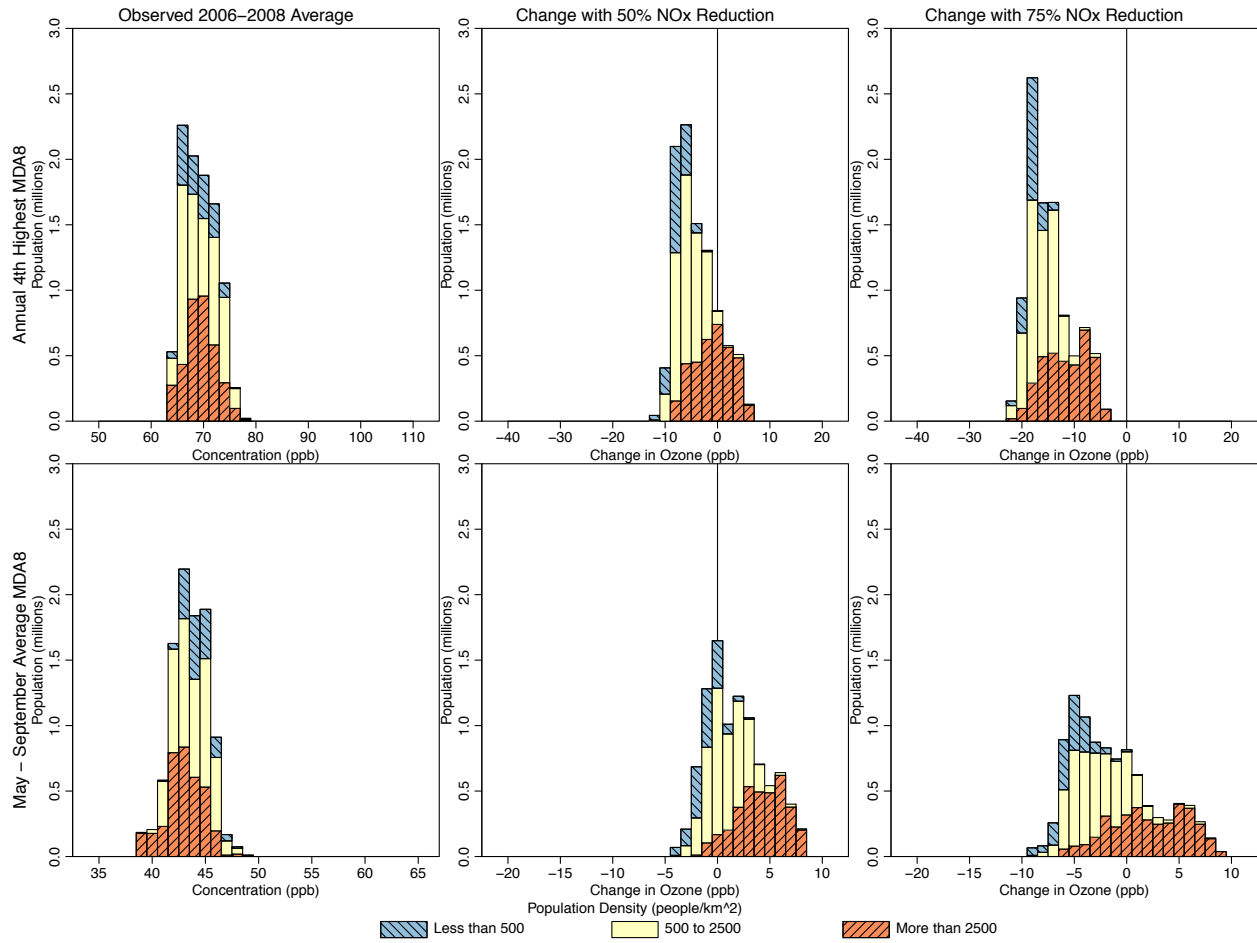


Figure 7.

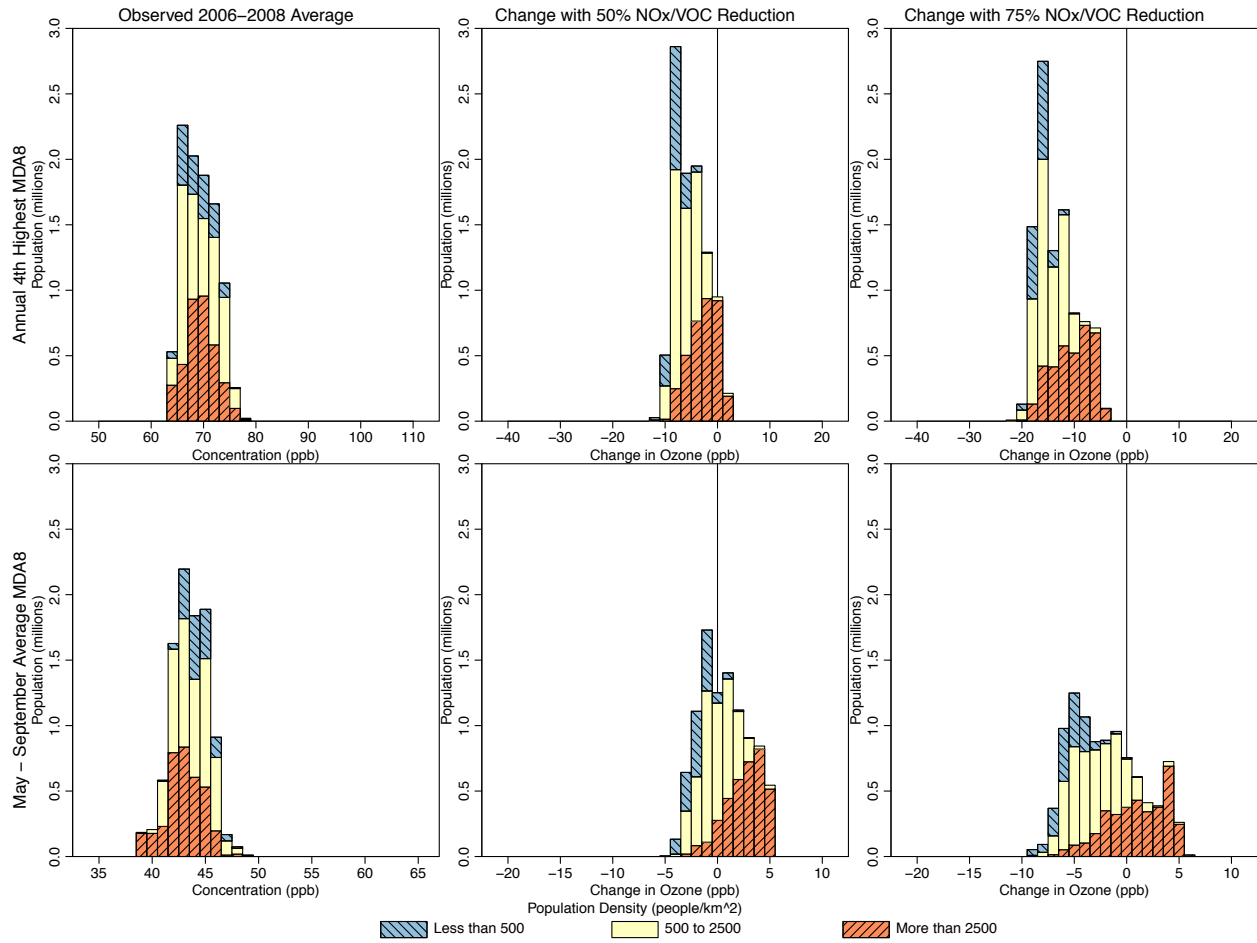


Figure 8.

